

## Large Excited-State Conformational Displacements Expedite Triplet Formation in a Small Conjugated Oligomer

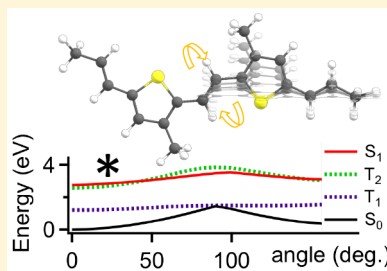
Benjamin D. Datko,<sup>†,§</sup> Maksim Livshits,<sup>†,§</sup> Zhen Zhang,<sup>†</sup> Yang Qin,<sup>†,ID</sup> Elena Jakubikova,<sup>‡,ID</sup> Jeffrey J. Rack,<sup>†,ID</sup> and John K. Grey\*,<sup>†,ID</sup>

<sup>†</sup>Department of Chemistry and Chemical Biology, University of New Mexico, Albuquerque, New Mexico 87131, United States

<sup>‡</sup>Department of Chemistry, North Carolina State University, Raleigh, North Carolina 27695, United States

### Supporting Information

**ABSTRACT:** Intersystem crossing in conjugated organic molecules is most conveniently viewed from pure electronic perspectives; yet, vibrational displacements may often drive these transitions. We investigate an alkyl-substituted thiénylene–vinylene dimer (dTV) displaying efficient triplet formation. Steady-state electronic and Raman spectra display large Stokes shifts ( $\sim 4000 \text{ cm}^{-1}$ ) involving high-frequency skeletal symmetric stretching modes ( $\sim 900$ – $1600 \text{ cm}^{-1}$ ) in addition to large displacements of low-frequency torsional motions ( $\sim 300$ – $340 \text{ cm}^{-1}$ ). Transient absorption spectroscopy reveals the emergence of distorted singlet ( $S_1$ ) and triplet signatures following initial vibrational relaxation dynamics that dominate spectral dynamics on time scales  $> 100 \text{ ps}$ , with the latter persisting on time scales up to ca. 7  $\mu\text{s}$ . Potential energy surfaces calculated along the dominant displaced out-of-plane torsional mode reveal shallow energy barriers for entering the triplet manifold from  $S_1$ . We propose that dTV is a good model system for understanding vibrational contributions to intersystem crossing events in related polymer systems.

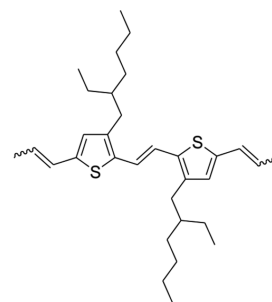


Spin-forbidden triplet excited states in conjugated organic molecules have a large bearing on functionality and performance at the materials level.<sup>1,2</sup> In most cases, intersystem crossing yields are small, and relaxation within the singlet manifold typically dominates excited-state dynamics.<sup>3</sup> On the other hand, conjugated heterocycles (e.g., thiophenes) often exhibit substantial triplet yields that vary significantly with size, conformation, and packing order.<sup>4–6</sup> Because there is now widespread interest in harvesting triplets to improve performance metrics of optoelectronic devices, such as solar cells,<sup>7,8</sup> comprehensive pictures of molecular electronic and structural factors governing transitions to and from the triplet manifold are needed.

Intersystem crossing events are most conveniently described from a pure electronic perspective that only considers vertical energies as inputs for estimating couplings and rate constants.<sup>9</sup> However, the role of vibrational motions in mediating triplet formation and relaxation is now receiving greater consideration.<sup>4,10</sup> There is also increased interest in potentially harnessing specific vibrational motions to regulate transitions between different spin state manifolds<sup>11</sup> although this topic has remained relatively unexplored.

Here, we investigate the roles of mode-specific vibrational displacements on triplet formation dynamics in an alkyl-substituted *trans*-thienylene–vinylene dimer (dTV; see Scheme 1), a small-molecule analogue of poly(thienylene–vinylenes) (PTV). PTV photophysics, though well studied, have remained controversial largely due to the short-lived nature of their excited states.<sup>12–14</sup> For example, dipole-forbidden midgap excited states (i.e.,  $2A_g$ ) have been invoked

**Scheme 1. Structure of the *trans*-Thienylene–Vinylene Dimer (dTV)**



to explain rapid excited-state relaxation and nonemissive behavior commonly observed in these systems.<sup>12,15,16</sup> This model was next amended by Musser et al. to include a singlet fission process within  $\sim 45 \text{ fs}$  followed by relaxation of the triplet pair to the  $2A_g$  state and subsequent decay to the ground electronic state.<sup>14</sup> However, Hu et al. demonstrated that fluorescence emission could be restored by dispersing a PTV derivative in a solid inert host, causing aggregates to dissociate.<sup>17</sup> Our group also recently observed rich Franck–Condon vibrational dynamics in aggregating PTVs, which promotes efficient nonradiative relaxation.<sup>18</sup> While a comprehensive photophysical model describing the interdependence

Received: February 20, 2019

Accepted: February 27, 2019

Published: February 27, 2019

on molecular structure is still lacking, minimizing complications from aggregation and heterogeneity effects is essential to obtain unambiguous views of photophysical pathways.<sup>19</sup> To this end, we demonstrate that dTV can serve as a model system for resolving vibrational contributions to intersystem crossing events in related molecules<sup>20</sup> and nonaggregating polymeric counterparts.

Figure 1 shows Raman spectra (a) and electronic absorption and fluorescence emission spectra (b) of dilute dTV solutions.

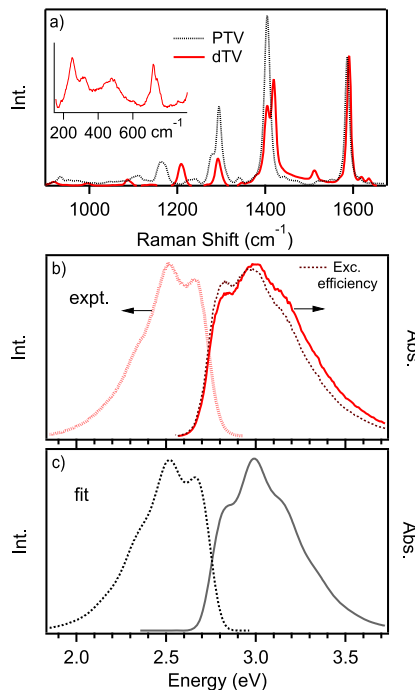


**Figure 1.** (a) Preresonant Raman spectra of dTV and a PTV analogue for comparison in the CC stretching region. Inset: enlarged low-frequency region of the dTV Raman spectrum. (b) Electronic absorption and fluorescence emission spectra of the dimer in dilute solution (o.d. < 0.1). (c) Simulated electronic spectra using Raman-active vibrations from (a).

Raman spectra were measured under off-resonance conditions (785 nm), showing activity in multiple skeletal vibrations. Comparison between Raman patterns of a related PTV derivative reveal similar features confirming intra- and inter-ring CC symmetric stretching vibrations that were assigned previously.<sup>21,22</sup> Both absorption and fluorescence emission spectra display a partially resolved vibronic progression with an average interval of  $\sim 1300$  cm<sup>-1</sup> representing the coalescence of multiple displaced skeletal modes. Stokes shifts of ca. 4000 cm<sup>-1</sup> are apparent, indicating large excited-state geometric distortions. We next used a simple undistorted harmonic oscillator model for up to nine modes (i.e., dominant displaced modes from Raman spectra) and a single electronic origin ( $E_{0-0}$ ) to simulate spectral line shapes in Figure 1b and obtained excellent agreement with experiment. Relative vibrational displacements were estimated using the short-time approximation ( $I_1/I_2 = \omega_1^2 \Delta_1^2 / \omega_2^2 \Delta_2^2$ ) from Raman intensities in Figure 1a, which are then scaled to the overall displacement determined from the overall absorption spectra widths (Table 1).<sup>23</sup> Importantly, it was necessary to include highly displaced low-frequency modes in order to obtain good agreement with the large observed Stokes shifts and vibronic

**Table 1.** Fit Parameters Used for dTV Absorption and Emission Spectra Simulations

mode (cm <sup>-1</sup> )	$\Delta$ (dimensionless)
1590	0.85
1420	0.6
1400	0.6
1290	0.55
1210	0.6
920	0.5
700	0.7
580	0.5
340	1.8
$E_{0-0}$ (cm <sup>-1</sup> )	22200
$\Gamma$ (cm <sup>-1</sup> )	200

line width broadening characteristics. Inspection of Raman spectra in the low-frequency regime reveals activity involving the vinylene group, especially out-of-plane torsional motions (ca. 300–340 cm<sup>-1</sup>). To this end, we used an effective frequency of 340 cm<sup>-1</sup> and varied the displacement to replicate experimental features that represents the dominant line width broadening contribution resulting in the shifts' spectral origins to higher (lower) energy for absorption (emission) transitions. Earlier spectroscopic investigations of phenylene–vinylene oligomers noted similar behavior at room temperature, where spectral broadening was attributed to large torsional displacements involving the vinylene group.<sup>24</sup> Fluorescence lifetime measurements in dilute solutions were also measured, revealing a single decay component of  $\sim 1.7$  ns, and excitation spectra overlap well with absorption line shapes, consistent with electronic transitions involving a single chromophore (data not shown).

The fact that highly displaced low-frequency torsional motions must be explicitly included in the vibronic analysis demonstrates that excited-state geometries are markedly different than the ground electronic state. We next measured transient absorption spectra of dTV dilute solutions to gain additional views into how these vibrational displacements impact photophysical branching ratios following relaxation of the Franck–Condon state. Figure 2a,b shows transient spectra of dTV in degassed chlorobenzene (CB) and dispersed in nujol, respectively. Spectral features are similar between the two samples, but dynamics change significantly depending on the surrounding medium. Two isosbestic points are labeled in Figure 2a,b by arrows that indicate the growth and decay of two species (ground-state and excited-state). Spectral components were obtained via multiexponential global kinetic analysis of the singular-value decomposition pump–probe data set, as well as single-wavelength multicomponent fits yielding identical time constants (see the Supporting Information).

In both media, spectra obtained at short time delays (several picoseconds) show a structured bleach feature strongly resembling the ground-state absorption line shape and two partially resolved excited-state absorption features with maxima at  $\sim 2.2$  and  $\sim 1.7$  eV. Not shown are the thermalization dynamics of the S<sub>1</sub> state, most likely involving the high-frequency skeletal vibrations associated with a time constant of  $\sim 250$  fs (see the Supporting Information). The  $\sim 2.2$  and  $\sim 1.7$  eV absorption transitions merge into a single excited-state absorption at  $\sim 2.5$  eV and a bleach feature that persists on microsecond time scales. Global kinetic analysis reveals time constants of  $260 \pm 100$  ps,  $1430 \pm 190$  ps, and  $6.7 \pm 0.2$   $\mu$ s in

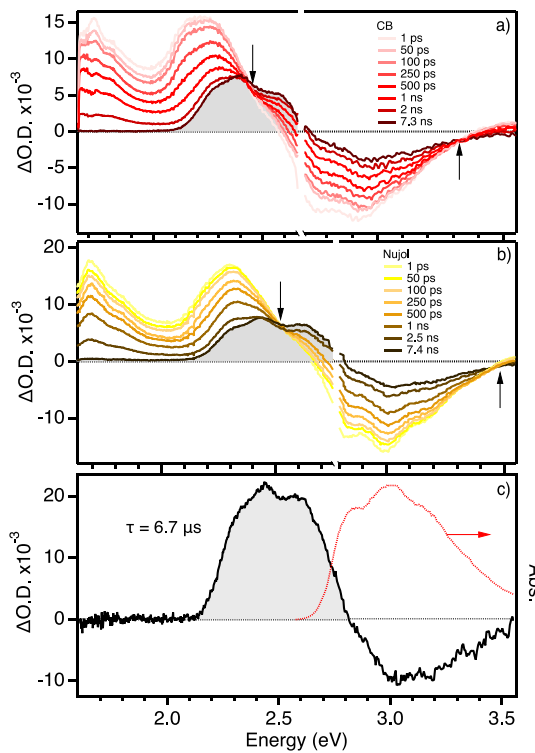


**Figure 2.** Broad-band transient absorption spectra of dTV in dilute CB (a) solutions and nujol (b) dispersions over various probe delay times. Pump excitation energies were typically  $\sim 2.6\text{--}2.8$  eV, and arrows depict resolved isosbestic points in the spectral dynamics. (c) Transient absorption spectrum of dTV from flash photolysis measurements in degassed dilute CB solution. A steady-state absorption spectrum (red dotted trace) is included for reference.

CB and  $210 \pm 40$  and  $1640 \pm 70$  ps in nujol. Nanosecond absorption spectra were not obtained for nujol dispersions, although the lifetime of the longer-lived component is expected to follow similar trends. In the presence of air, the long-time constant in CB decreases to  $\sim 200$  ns (see the Supporting Information). On the basis of the lifetime range and sensitivity to the environment, the long-lived component can be assigned as relaxation of the lowest-energy triplet ( $T_1$ ) to the ground electronic state ( $S_0$ ), whereas assignments of faster dynamics are less straightforward.

To further home-in on factors involved in transitioning to the triplet manifold, we turned to density functional theory (DFT) simulations. Figure 3 displays HOMO and LUMO isosurfaces ( $0.03$  e/Å $^3$ ) of the dTV molecule calculated at the B3LYP/6-31G(d) level of theory in vacuum with the branched ethyl–hexyl groups replaced by methyl groups. The ground-state ( $S_0$ ) geometry was optimized in  $C_{2h}$  symmetry, and time-dependent DFT (TD-DFT) simulations at the same level of theory were employed to obtain the five lowest-energy excited states utilizing the fully optimized  $S_0$  as a reference state. Importantly, the transition with the largest oscillator strength (1.3) corresponded to 100% HOMO  $\rightarrow$  LUMO character with vertical excitation energies of 2.75 eV, in excellent agreement with the HOMO–LUMO energy gap and experiment (see the Supporting Information).

We next calculated potential energy surfaces for the lowest-energy singlet ( $S_0, S_1, S_2$ ) and triplet ( $T_1, T_2, T_3$ ) states along the most prominent displaced torsional mode, i.e., the effective 340 cm $^{-1}$  mode (see the Supporting Information). Compar-

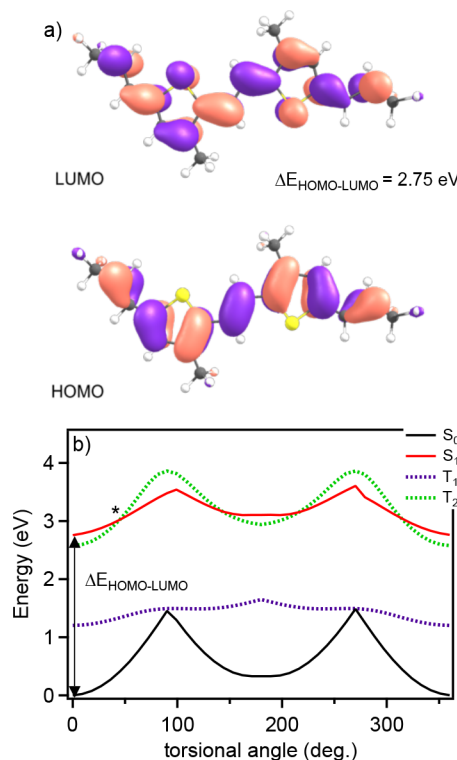


**Figure 3.** (a) HOMO and LUMO isosurfaces ( $0.03$  e/Å $^3$ ) for the dTV model compound. (b) Potential energy surfaces for  $S_0$ ,  $S_1$ ,  $T_1$ , and  $T_2$  states calculated using the torsional displacement coordinate. The HOMO–LUMO energy gap is indicated, and the asterisk denotes the crossing between the distorted  $S_1$  and  $T_2$  excited states (see the text).

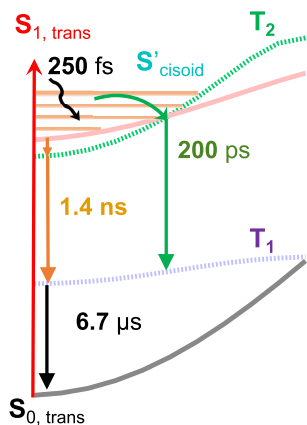
ison with simulated Raman spectra confirms that modes in this low-frequency region involve out-of-plane dTV torsional motions that are known to exert a large influence on the photophysics of related molecules.<sup>25–27</sup> Potential energy surfaces are shown in Figure 3b, revealing large energetic barriers for converting to the cis form of dTV in  $S_0$  (the full procedure for calculating potentials is included in the Supporting Information). These barriers are substantially relaxed in the  $S_1$  state, although the trans form remains the lowest in energy by  $\sim 1$  eV. We also performed TD-DFT simulations by optimizing the dTV structure in the  $S_1$  state and found a small decrease ( $\sim 0.17$  eV) in the locations of potential minima compared to vertically projecting the ground-state geometry (see the Supporting Information).

It is useful to point out the predicted intersection between  $S_1$  and a higher-energy triplet state,  $T_2$ , corresponding to a distortion of  $\sim 50^\circ$  along the torsional coordinate. These profiles indicate that the  $T_2$  state is the likely conduit for entering the triplet manifold due to minimization of the singlet–triplet energy gap.<sup>9,28</sup> Interestingly, earlier work on related compounds proposed that intersystem crossing requires large conformational deformations leading to isostructural cisoid singlet and triplet excited states.<sup>27</sup> Moreover, recent nonadiabatic excited-state simulations of model thiophene oligomers reported intersystem crossing via the  $S_1$ – $T_2$  intersection as the principal relaxation channel.<sup>29</sup> This process was also found to be driven by inter-ring torsional motions and ring-opening deformations that becomes impeded in larger molecules. These authors predicted that the initial intersystem crossing time constant to be  $\sim 140$  ps followed by relaxation to

the lowest-energy  $T_1$  state occurred on much longer time scales ( $\sim 1.3$  ns) and with eventual recovery to  $S_0$  ( $\sim 7$   $\mu$ s).<sup>29</sup>

On the basis of predictions from DFT simulations and prior work on related molecules,<sup>27–29</sup> we assign the ca. 200 ps decay constant in both media to transitions involving a distorted (cisoid)  $S_1$  state, consistent with the broader spectral line shape at  $\sim 2.2$  eV (see the *Supporting Information*). This geometry enables facile intersystem crossing to the nearly isoenergetic  $T_2$  state with the same geometry due to minimization of the singlet–triplet energy gap. A caveat of this assignment is that it requires excess excitation energy to surmount the potential energy barrier of torsional motion to access the cisoid  $S_1$  state. Slower transitions to  $T_1$  are also possible, probably involving the relaxed  $S_1$  state that we assign as the ca. 1.4 ns dominated by the  $\sim 1.7$  eV absorption feature (see the *Supporting Information*). The appearance of the prominent isosbestic point in transient absorption spectra (Figure 2) demonstrates that both pathways to  $T_1$  are operative. However, conformational distortions expedite the intersystem crossing transition, which is consistent with high sensitivity of associated dynamics to the surrounding medium. Scheme 2 illustrates the proposed relaxation mechanisms in dTV.

**Scheme 2. Proposed Excited-State Relaxation Pathways of dTV**



Although earlier work demonstrated the prevalence of ring opening and ring deformations as possible channels for accessing the triplet manifold, it is likely that such mechanisms would result in the appearance of distinct photoproducts (e.g., cis conformers).<sup>29</sup> These forms should possess markedly different absorption energies and line shapes over time. No significant changes in absorption line shapes were observed (see the *Supporting Information*), indicating that intersystem crossing and relaxation within the triplet manifold dominate relaxation dynamics.

We have demonstrated the importance of large conformational displacements in transitioning into the triplet manifold in a small thiénylene–vinylene oligomer. Our results offer additional perspectives of triplet signatures appearing on fast time scales in related polymer systems that are usually interpreted on the basis of multistep processes involving pure electronic states. The fact that triplet signatures vanish in aggregating polymer analogues of dTV and are instead dominated by nonradiative relaxation involving many vibrational modes demonstrates that specific geometric distortions govern intersystem crossing in these systems. Furthermore,

controlling aggregation characteristics as well as vibrational displacements may be accomplished straightforwardly by simply varying processing approaches.

## EXPERIMENTAL METHODS

dTV was synthesized and characterized according to procedures described in the *Supporting Information*. Absorption and fluorescence spectra were measured from dilute dTV solutions (CB, o.d.  $< 0.1$ ) and corrected for instrument response. Fluorescence lifetimes were recorded using time-correlated single-photon counting techniques, and lifetimes were obtained with an iterative deconvolution procedure. Raman spectra of both solutions and solids were generated using off-resonance excitation (785 nm) on a microscope-based spectrometer. Transient absorption spectroscopy measurements were performed on degassed dTV CB solutions and nujol dispersions. The full description of the apparatus is provided in the *Supporting Information*. Briefly, pump–probe excitations were generated with a Ti:sapphire regenerative amplifier (Spectra Physics Solstice, 7 mJ, 800 nm) used to pump an optical parametric amplifier (Light Conversion Topas Prime, 4.7 mJ). A white light probe continuum was produced with a CaF<sub>2</sub> window and delayed in time via a multipass retroreflector. The pump and probe beams were overlapped in a pseudo-collinear geometry, and pump fluences were  $< 1$  mJ/cm<sup>2</sup>. Absorption signals were collected and dispersed in an optical fiber-based spectrograph (Oriel). DFT calculations were performed using Gaussian 09 at the B3LYP/6-31(d) level.<sup>30</sup> TD-DFT simulations and potential energy surface calculations were according to the procedure described in the *Supporting Information*.

## ASSOCIATED CONTENT

### Supporting Information

The Supporting Information is available free of charge on the ACS Publications website at DOI: [10.1021/acs.jpclett.9b00495](https://doi.org/10.1021/acs.jpclett.9b00495).

Synthetic procedure and characterization of dTV molecules, methodology of DFT calculations and coordinates, vibrational frequencies and activities, TD-DFT excitation energies, and global fitting model of absorption transients ([PDF](#))

## AUTHOR INFORMATION

### Corresponding Author

\*E-mail: [jkgrey@unm.edu](mailto:jkgrey@unm.edu).

### ORCID

Yang Qin: [0000-0002-5764-8137](https://orcid.org/0000-0002-5764-8137)

Elena Jakubikova: [0000-0001-7124-8300](https://orcid.org/0000-0001-7124-8300)

Jeffrey J. Rack: [0000-0001-6121-879X](https://orcid.org/0000-0001-6121-879X)

John K. Grey: [0000-0001-7307-8894](https://orcid.org/0000-0001-7307-8894)

### Author Contributions

<sup>§</sup>B.D.D. and M.L. contributed equally to this work.

### Notes

The authors declare no competing financial interest.

## ACKNOWLEDGMENTS

J.K.G. acknowledges support from the National Science Foundation (CHE-1506558). J.J.R. acknowledges the National Science Foundation (CHE-1602240) and the University of New Mexico for financial support. E.J. acknowledges support

from the National Science Foundation (CHE-1554855). Y.Q. acknowledges support from the National Science Foundation (DMR-1453083) for this research.

## ■ REFERENCES

- (1) Scholes, G. D. Long-Range Resonance Energy Transfer in Molecular Systems. *Annu. Rev. Phys. Chem.* **2003**, *54*, 57–87.
- (2) Ohkita, H.; Cook, S.; Astuti, Y.; Duffy, W.; Tierney, S.; Zhang, W.; Heeney, M.; McCulloch, I.; Nelson, J.; Bradley, D. D. C.; et al. Charge Carrier Formation in Polythiophene/Fullerene Blend Films Studied by Transient Absorption Spectroscopy. *J. Am. Chem. Soc.* **2008**, *130*, 3030–3042.
- (3) Fazzi, D.; Barbatti, M.; Thiel, W. Modeling Ultrafast Exciton Deactivation in Oligothiophenes Via Nonadiabatic Dynamics. *Phys. Chem. Chem. Phys.* **2015**, *17*, 7787–7799.
- (4) Siegert, S.; Vogeler, F.; Marian, C. M.; Weinkauf, R. Throwing Light on Dark States of A-Oligothiophenes of Chain Lengths 2 to 6: Radical Anion Photoelectron Spectroscopy and Excited-State Theory. *Phys. Chem. Chem. Phys.* **2011**, *13*, 10350–10363.
- (5) Koelle, P.; Schnappinger, T.; de Vivie-Riedle, R. Deactivation Pathways of Thiophene and Oligothiophenes: Internal Conversion Versus Intersystem Crossing. *Phys. Chem. Chem. Phys.* **2016**, *18*, 7903–7915.
- (6) Thomas, A. K.; Garcia, J. A.; Ulibarri-Sanchez, J.; Gao, J.; Grey, J. K. High Intra-Chain Order Promotes Triplet Formation from Recombination of Long-Lived Polarons in Poly(3-Hexylthiophene) J-Aggregate Nanofibers. *ACS Nano* **2014**, *8*, 10559–10568.
- (7) Xia, J.; Sanders, S. N.; Cheng, W.; Low, J. Z.; Liu, J.; Campos, L. M.; Sun, T. Singlet Fission: Progress and Prospects in Solar Cells. *Adv. Mater.* **2017**, *29*, 1601652.
- (8) Rao, A.; Friend, R. H. Harnessing Singlet Exciton Fission to Break the Shockley-Queisser Limit. *Nat. Rev. Mater.* **2017**, *2*, 17063.
- (9) Mai, S.; Marquetand, P.; Gonzalez, L. A General Method to Describe Intersystem Crossing Dynamics in Trajectory Surface Hopping. *Int. J. Quantum Chem.* **2015**, *115*, 1215–1231.
- (10) Penfold, T. J.; Gindensperger, E.; Daniel, C.; Marian, C. M. Spin-Vibronic Mechanism for Intersystem Crossing. *Chem. Rev.* **2018**, *118*, 6975–7025.
- (11) Renaud, N.; Grozema, F. C. Intermolecular Vibrational Modes Speed up Singlet Fission in Perylenediimide Crystals. *J. Phys. Chem. Lett.* **2015**, *6*, 360–365.
- (12) Olejnik, E.; Pandit, B.; Basel, T.; Lafalce, E.; Sheng, C. X.; Zhang, C.; Jiang, X.; Vardeny, Z. V. Ultrafast Optical Studies of Ordered Poly(3-Thienylene-Vinylene) Films. *Phys. Rev. B: Condens. Matter Mater. Phys.* **2012**, *85*, 235201/1–235201/6.
- (13) Ozaki, M.; Ehrenfreund, E.; Benner, R. E.; Barton, T. J.; Yoshino, K.; Vardeny, Z. V. Dispersion of Resonant Raman Scattering in  $\pi$ -Conjugated Polymers: Role of the Even Parity Excitons. *Phys. Rev. Lett.* **1997**, *79*, 1762–1765.
- (14) Musser, A. J.; Al-Hashimi, M.; Maiuri, M.; Brida, D.; Heeney, M.; Cerullo, G.; Friend, R. H.; Clark, J. Activated Singlet Exciton Fission in a Semiconducting Polymer. *J. Am. Chem. Soc.* **2013**, *135*, 12747–12754.
- (15) Frolov, S. V.; Vardeny, Z. V. Picosecond Strain Waves in PTV. *Synth. Met.* **1997**, *84*, 905–906.
- (16) Liess, M.; Jeglinski, S.; Lane, P. A.; Vardeny, Z. V. A Three Essential States Model for Electroabsorption in Nonluminescent  $\pi$ -Conjugated Polymers. *Synth. Met.* **1997**, *84*, 891–892.
- (17) Hu, Z.; Adachi, T.; Lee, Y.-G.; Haws, R. T.; Hanson, B.; Ono, R. J.; Bielawski, C. W.; Ganesan, V.; Rossky, P. J.; Vanden Bout, D. A. Effect of the Side-Chain-Distribution Density on the Single-Conjugated-Polymer-Chain Conformation. *ChemPhysChem* **2013**, *14*, 4143–4148.
- (18) Datko, B. D.; Livshits, M. Y.; Zhang, Z.; Portlock, D.; Qin, Y.; Rack, J. J.; Grey, J. K. Unravelling the Enigma of Ultrafast Excited State Relaxation in Non-Emissive Aggregating Conjugated Polymers. *Phys. Chem. Chem. Phys.* **2018**, *20*, 22159–22167.
- (19) DiCesare, N.; Belletete, M.; Marrano, C.; Leclerc, M.; Durocher, G. Intermolecular Interactions in Conjugated Oligothiophenes. 1. Optical Spectra of Terthiophene and Substituted Terthiophenes Recorded in Various Environments. *J. Phys. Chem. A* **1999**, *103*, 795–802.
- (20) Elfers, N.; Lyskov, I.; Spiegel, J. D.; Marian, C. M. Singlet Fission in Quinoidal Oligothiophenes. *J. Phys. Chem. C* **2016**, *120*, 13901–13910.
- (21) Louarn, G.; Mevellec, J. Y.; Lefrant, S.; Buisson, J. P.; Fichou, D.; Teulade-Fichou, M. P. Raman Study of A-Oligothiophenes and Model Compounds of Poly(Thienylenevinylene). *Synth. Met.* **1995**, *69*, 351–352.
- (22) Mevellec, J. Y.; Buisson, J. P.; Lefrant, S.; Eckhard, H.; Jen, K. Y. Theoretical Analysis of the Raman Spectra of PTV and PFV. *Synth. Met.* **1990**, *35*, 209–213.
- (23) Heller, E. J.; Sundberg, R.; Tannor, D. Simple Aspects of Raman Scattering. *J. Phys. Chem.* **1982**, *86*, 1822–1833.
- (24) Gierschner, J.; Mack, H.-G.; Lüer, L.; Oelkrug, D. Fluorescence and Absorption Spectra of Oligophenylenes: Vibronic Coupling, Band Shapes, and Solvatochromism. *J. Chem. Phys.* **2002**, *116*, 8596–8609.
- (25) Lin, J. B.; Jin, Y.; Lopez, S. A.; Druckerman, N.; Wheeler, S. E.; Houk, K. N. Torsional Barriers to Rotation and Planarization in Heterocyclic Oligomers of Value in Organic Electronics. *J. Chem. Theory Comput.* **2017**, *13*, 5624–5638.
- (26) Millefiori, S.; Alparone, A.; Millefiori, A. Conformational Properties of Thiophene Oligomers. *J. Heterocycl. Chem.* **2000**, *37*, 847–853.
- (27) Zimmerman, A. A.; Orlando, C. M.; Gianni, M. H.; Weiss, K. Concentration Effects in Photochemical Cis-Trans Isomerization. Difurylethylene and Dithienylethylene. *J. Org. Chem.* **1969**, *34*, 73–77.
- (28) Mai, S.; Marquetand, P.; Gonzalez, L. Intersystem Crossing Pathways in the Noncanonical Nucleobase 2-Thiouracil: A Time-Dependent Picture. *J. Phys. Chem. Lett.* **2016**, *7*, 1978–1983.
- (29) Schnappinger, T.; Koelle, P.; Marazzi, M.; Monari, A.; Gonzalez, L.; de Vivie-Riedle, R. Ab Initio Molecular Dynamics of Thiophene: The Interplay of Internal Conversion and Intersystem Crossing. *Phys. Chem. Chem. Phys.* **2017**, *19*, 25662–25670.
- (30) Frisch, M. J.; Trucks, G. W.; Schlegel, H. B.; Scuseria, G. E.; Robb, M. A.; Cheeseman, J. R.; Scalmani, G.; Barone, V.; Mennucci, B.; Petersson, G. A. *Gaussian 09*, revision C.01; Gaussian, Inc.: Wallingford, CT, 2009.